

# Luminescent Cyclometalated Platinum(II) Complex Forms Emissive Intercalating Adducts with Double-Stranded DNA and RNA: Differential Emissions and Anticancer Activities\*\*

Taotao Zou, Jia Liu, Ching Tung Lum, Chensheng Ma, Ruth Chau-Ting Chan, Chun-Nam Lok, Wai-Ming Kwok, and Chi-Ming Che\*

**Abstract:** Luminescent metallo-intercalators are potent biosensors of nucleic acid structure and anticancer agents targeting DNAs. There are few examples of luminescent metallo-intercalators which can simultaneously act as emission probes of nucleic acid structure and display promising anticancer activities. Herein, we describe a luminescent platinum(II) complex,  $[Pt(C^{\wedge}N^{\wedge}N)(C\equiv NtBu)]ClO_4$  (**1a**,  $HC^{\wedge}N^{\wedge}N=6$ -phenyl-2,2'-bipyridyl), that intercalates between the nucleobases of nucleic acids, accompanied by an increase in emission intensity and/or a significant change in the maximum emission wavelength. The changes in emission properties measured with double-stranded RNA (dsRNA) are different from those with dsDNA used in the binding reactions. Complex **1a** exhibited potent anticancer activity towards cancer cells *in vitro* and inhibited tumor growth in a mouse model. The stabilization of the topoisomerase I–DNA complex with resulting DNA damage by **1a** is suggested to contribute to its anticancer activity.

It has been established that luminescent metal complexes bind DNA through covalent bonding and/or non-covalent interactions, such as intercalation and major or minor groove binding interactions.<sup>[1]</sup> The non-covalent interactions have been used to develop luminescent probes for the detection of nucleic acids (NAs), including mismatched DNA and G-quadruplexes,<sup>[1c,i,2]</sup> and can potentially confer therapeutic properties, such as anticancer activities. Although luminescent metal complexes have been used extensively as probes for DNA,<sup>[1c,i,2]</sup> related studies on double-stranded RNA (dsRNA) are underdeveloped, despite the pivotal role that dsRNA plays in various processes, such as RNA trafficking, editing, and maturation, as well as RNA interference and interferon antiviral response.<sup>[3]</sup> Recent efforts to develop dsRNA probes have focused mainly on proteins and small organic molecules with specific targeting moieties.<sup>[3d,h,4]</sup>

Various studies revealed that  $\pi$ -stacking interactions between adjacent nucleobases of natural B-form duplex DNA could lead to the formation of emissive excimer/excplex species<sup>[5]</sup> and facilitate effective charge transfer along DNA bases.<sup>[6]</sup> Some organic intercalators are known to undergo  $\pi$  interactions with nucleobase(s) of modified dsDNA to form emissive exciplexes,<sup>[7]</sup> including a pyrene-modified oligonucleotide that can bind to both its complementary DNA and RNA sequences.<sup>[7a]</sup> Metal complexes can form emissive exciplexes<sup>[8b,c]</sup> or non-emissive exciplexes.<sup>[8b,f,j]</sup> Although there have been numerous examples of non-emissive exciplexes formed between metal complexes and DNA,<sup>[8d,e,h]</sup> only one metal complex displays exciplex emission in which the emission maximum ( $\lambda_{max}$ ) undergoes a distinct shift upon intercalation with calf thymus DNA (ctDNA).<sup>[9]</sup> In recent years, the chemistry and biology of luminescent platinum complexes has been investigated, including their binding interactions with nucleic acid structures<sup>[8g,i,j]</sup> and their potential therapeutic applications.<sup>[8i]</sup> As dsRNA features an A-form double helix in which the spatial geometry of nucleobases is different to that of the B-form duplex of dsDNA,<sup>[10]</sup> we envisage the feasibility to differentiate between dsRNA and dsDNA by using the electronic interactions between nucleobases and metallo-intercalators in the excited states. Non-covalent binding interactions between metallo-intercalators and nucleic acids could also confer therapeutic activity.<sup>[11]</sup> Some examples of DNA intercalating agents perturb DNA topoisomerase (Topo) function by stabilization of the covalent Topo–DNA complex, resulting in excessive DNA strand breaks that trigger programmed cell death of cancer cells.<sup>[12]</sup> Herein, we describe the platinum(II)

[\*] T. Zou,<sup>[4]</sup> Dr. J. Liu,<sup>[4]</sup> Dr. C. T. Lum, Dr. C. Ma,<sup>[5]</sup> Dr. C.-N. Lok, Prof. Dr. C.-M. Che

State Key Laboratory of Synthetic Chemistry  
Institute of Molecular Functional Materials  
Chemical Biology Centre and  
Department of Chemistry, The University of Hong Kong  
Pokfulam Road, Hong Kong (China)  
E-mail: cmche@hku.hk

Prof. Dr. C.-M. Che  
HKU Shenzhen Institute of Research and Innovation  
Shenzhen 518053 (China)

R. C.-T. Chan, Dr. W.-M. Kwok  
Department of Applied Biology and Chemical Technology  
The Hong Kong Polytechnic University  
Hung Hom, Kowloon, Hong Kong (China)

[†] Current address: School of Chemistry and Chemical Engineering  
Shenzhen University (China)

[‡] These authors contributed equally to this work.

[\*\*] This work was supported by the University Grants Committee of the HKSAR of China (Area of Excellence Scheme AoE/P-03/08), the National Key Basic Research Program of China (2013CB834802), the Hong Kong Research Grant Council (HKU 700812P), and Special Equipment Grant of UGC (SEG\_HKU02) for MS analysis. We thank Drs. C.-H. Leung, D.-L. Ma, R. W.-Y. Sun for constructive input, and Prof. Anderson Wong for help on radioisotope experiments.

Supporting information for this article is available on the WWW under <http://dx.doi.org/10.1002/anie.201405384>.

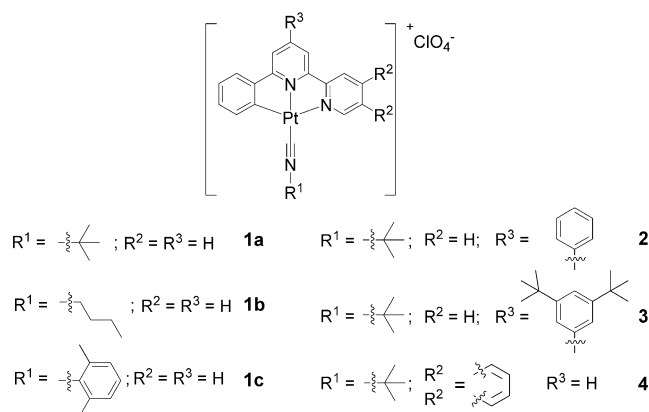


**Figure 1.** Structural formula of platinum(II) pincer complexes **1 a–c** and **2–4**.

complex  $[\text{Pt}(\text{C}^{\wedge}\text{N}^{\wedge}\text{N})(\text{C}\equiv\text{N}t\text{Bu})]\text{ClO}_4$  (**1a**,  $\text{HC}^{\wedge}\text{N}^{\wedge}\text{N} = 6$ -phenyl-2,2'-bipyridyl, Figure 1),<sup>[13]</sup> which is a metallo-intercalator that forms emissive intercalating adducts with emission properties sensitive to the structure of NAs. Complex **1a** also strongly and selectively inhibits cancer cells growth in vitro and suppresses tumor growth in vivo.

The synthetic procedures and characterization data for platinum(II) complexes **1–4** (Figure 1) are given in the Supporting Information. Treatment of the platinum(II) complexes, such as **1a**, with glutathione (GSH, 2 mM) in DMSO/Tris buffered solution (1:9 v/v) did not reveal significant UV/Vis absorption spectral changes over a 24 h period. ESI-MS analyses showed that **1a** was stable in solutions containing different amino acids/peptides (e.g. GSH, Lys, Arg, His) and DNA bases (e.g. A, G, T), as no new species were detected after 12–24 h incubation times (Figure S1 in the Supporting Information). Inductively coupled plasma mass spectrometry (ICP-MS) revealed that the quantity of unbound (non-covalent) platinum recovered in the supernatant after acetone precipitation of proteins in fetal bovine serum was more than 85% after 24 h incubation (Figure S2).

The binding constant  $K$  of **1a** with ctDNA at 298 K determined by a UV/Vis absorption titration experiment is  $1.0 \times 10^6 \text{ M}^{-1}$  (Figure S3). The viscosity of a ctDNA solution increases upon addition of **1a** (Figure S4), which is attributed to the insertion of **1a** into the space between stacked base pairs (intercalation), leading to an increase in the apparent molecular length of DNA.<sup>[14]</sup> A  $^1\text{H}$  NMR titration experiment of a short oligomer  $\text{d}(\text{CA}_2\text{TC}_2\text{G}_2\text{AT}_2\text{G})_2$  in the presence of **1a** showed that the resonance signals of the oligomer in the region  $\delta = 7.0\text{--}8.2$  ppm broaden and undergo an upfield shift (Figure S5), which is suggestive of an intercalative binding mode.<sup>[15]</sup> Complex **1a** intercalates more strongly into AT-rich DNA  $[\text{d}(\text{ATA}_2\text{T}_2\text{A}_3\text{T}_3\text{A}_4\text{T}_4\text{A}_2)_2]$  than GC-rich DNA  $[\text{d}(\text{CGC}_2\text{G}_2\text{C}_3\text{G}_3\text{C}_4\text{G}_4\text{C}_2)_2]$ . This preference is indicated by the greater increase in viscosity for AT-rich DNA than for GC-rich DNA upon addition of **1a** (Figure S6).

In contrast its emission maximum, the emission quantum yield of **1a** is sensitive to the solvent. The emission quantum yields of **1a** (20  $\mu\text{M}$ ) in degassed  $\text{CH}_2\text{Cl}_2$ ,  $\text{CHCl}_3$ ,  $\text{CH}_3\text{CN}$ , and DMSO, are 0.63 ( $\lambda_{\text{max}} = 527 \text{ nm}$ ,  $\tau = 11.5 \mu\text{s}$ ), 0.43 ( $\lambda_{\text{max}} = 522 \text{ nm}$ ,  $\tau = 4.6 \mu\text{s}$ ), 0.097 ( $\lambda_{\text{max}} = 526 \text{ nm}$ ,  $\tau = 2.2 \mu\text{s}$ ), and less

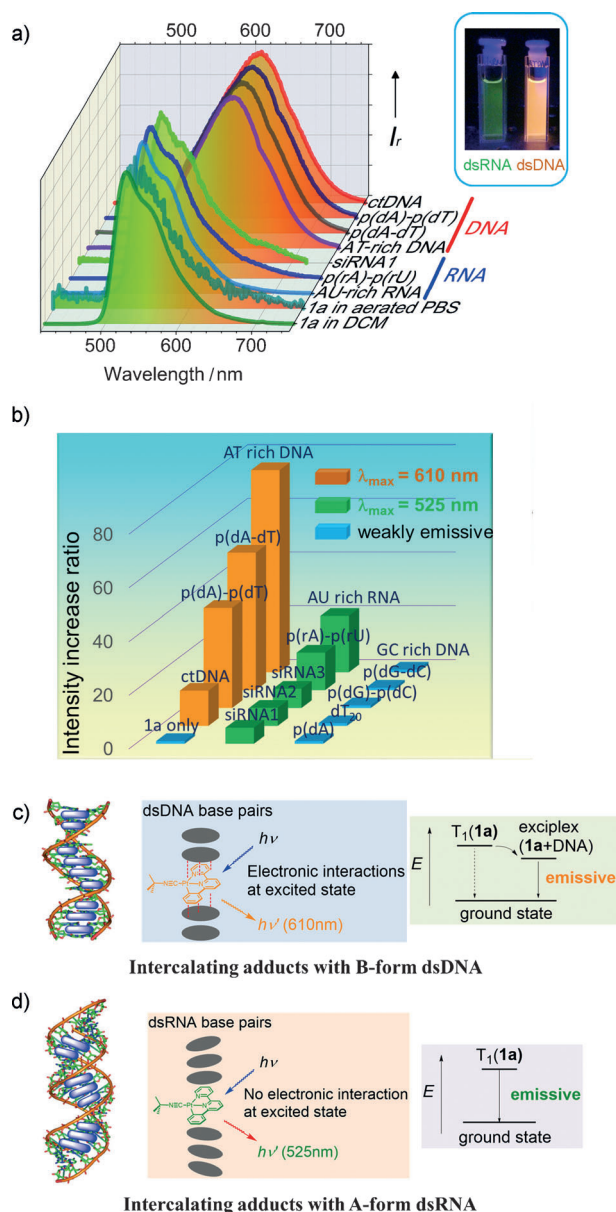


**Figure 2.** a) Normalized emission spectra of **1a** (20  $\mu\text{M}$ ) in  $\text{CH}_3\text{CN}/\text{PBS}$  (1:9 v/v) containing different NAs or in  $\text{CH}_2\text{Cl}_2$  ( $\lambda_{\text{ex}} = 350 \text{ nm}$ ). Inset: photos of **1a** (20  $\mu\text{M}$ ) with AU-rich dsRNA and AT-rich dsDNA under  $\lambda = 365 \text{ nm}$  UV irradiation. b) Emission peak intensity of **1a** (20  $\mu\text{M}$ ) upon addition of different NAs (10  $\mu\text{M}$ ). Emission intensity denoted by green ( $\lambda = 525 \text{ nm}$ ) and orange ( $\lambda = 610 \text{ nm}$ ) bars, with the blue bar indicating weak emission. c) Proposed binding interactions of **1a** with dsDNA and d) **1a** with dsRNA in the excited state. Energy-level diagrams showing the nature of the emissive excited state (c, d).

than  $10^{-3}$ , respectively (Figure S7 and Table S1 in the Supporting Information). Complex **1a** is weakly emissive in aerated PBS/ $\text{CH}_3\text{CN}$  solution (19:1 v/v, PBS = phosphate buffered saline) with an emission maximum at approximately  $\lambda = 525 \text{ nm}$  (Figure 2a). In the presence of ctDNA or AT-rich DNA, the  $\lambda_{\text{max}}$  band is red-shifted to  $\lambda = 610 \text{ nm}$  and the emission intensity increases by a factor of 175 and 200 when  $[\text{DNA}]/[\text{1a}] = 1.2$  and 1.9, respectively (Figures S8a,b). As there is only a 5 nm shift in the emission maximum of **1a** when the solvent is changed between  $\text{CH}_2\text{Cl}_2$ ,  $\text{CHCl}_3$ , and  $\text{CH}_3\text{CN}$ ,

the 85 nm emission maximum red shift (from  $\lambda = 525$  nm to 610 nm) upon binding of **1a** to DNA (by intercalation) cannot be attributed to solely the effect of the medium.<sup>[9]</sup> The formation of a new emissive excited-state species is suggested based on the following considerations: 1) the excitation spectra of the emission of **1a** in the presence of poly(dA-dT) (p(dA-dT)) or ctDNA ( $\lambda_{em} = 610$  nm) are similar to the absorption spectrum of **1a** (Figure S9), showing no additional band, a slight red shift in peak maximum, and only minor variation in intensity; 2) the space between adjacent base pairs is too small to allow formation of aggregates inside; 3) the excimer emission of **1a**, through intermolecular  $\pi$ -stacking interactions of the C<sup>^</sup>N<sup>^</sup>N<sup>^</sup> ligands, occurs at a comparable energy ( $\lambda_{max} = 627$  nm);<sup>[16]</sup> 4) the emission and photophysical properties of the intercalating adduct are sensitive to the nucleic acid structures. For example, in contrast to ctDNA or AT-rich DNA, the addition of dsRNA of poly(rA)-poly(rU) (p(rA)-p(rU)) to **1a** in PBS buffer leads to an emission enhancement but with no change in the  $\lambda_{max}$  band (Figure 2a). Nanosecond time-resolved emission (ns-TRE) spectroscopic experiments revealed a fast decay signal with  $\tau = 52$  ns (Figure S10a,g), similar to that of **1a** alone in PBS buffer (Figure S10b,g). This signal is attributed to the triplet excited state of unbound complex **1a** ( $T_f$ ) which is subject to O<sub>2</sub> quenching. At the same time, there is a slower decay process with an excited-state lifetime of  $\tau = 8.5$   $\mu$ s, that is ascribed to the triplet excited state of **1a** which is intercalated between the p(rA)-p(rU) bases ( $T_c$ ). In the presence of ctDNA or p(dA-dT), ns-TRE spectroscopy showed an emission band with a maximum of approximately  $\lambda = 610$  nm and an excited-state lifetime on the microsecond timescale (Figure S10d,e,h). The emission decay profile is composed of a fast component ( $\tau = 52$  ns, attributed to  $T_f$ ; Figure S10h) and a slower component ( $\tau = 2.7$   $\mu$ s). Thus, in both the cases of ctDNA and p(dA-dT), the longer lifetime decay signal (2.7  $\mu$ s), the significant red shift in emission energy (from  $\lambda = 525$  nm to 610 nm), and the fact that the emission centered at  $\lambda = 610$  nm is broad and structureless, lend support to the formation of an emissive exciplex, with a triplet excited state denoted  $T_c$ . This exciplex is presumably stabilized through an electronic binding interaction between the triplet excited state of **1a** and an A/T base in ctDNA or p(dA-dT), as depicted in Figure 2c. Meanwhile, the TRE decay (Figure S10h) is also consistent with the different levels of increased emission intensity detected upon binding of **1a** with ctDNA and p(dA-dT); the ratio of weakly emissive  $T_f$  to strongly emissive  $T_c$  in the case of ctDNA is much larger than that in the case of p(dA-dT). Addition of p(dG-dC) to **1a** results in the detection of only a fast decay signal with  $\tau = 52$  ns (Figure S10c,g) that is attributed to the formation of  $T_f$ ; presumably the interaction between **1a** and p(dG-dC) is weak. Among the various dsDNA sequences investigated (specifically ctDNA, p(dA)-p(dT), p(dA-dT), AT-rich DNA, p(dG-dC), p(dG)-p(dC), GC-rich DNA and single-stranded DNA of poly(dA) and oligo(dT<sub>20</sub>); Figure 2b), the AT-rich DNA gave the highest enhancement of emission intensity upon its binding reaction with **1a**. Experiments revealed that **1a** could be used to detect AT-rich DNA by emission

measurement at concentrations as low as 100 nM in PBS (see the Supporting Information).

The emissive exciplex formed between [Pt(dppz)-(tN<sup>^</sup>C)]CF<sub>3</sub>SO<sub>3</sub> (dppz = dipyrido[3,2-*a*:2',3'-*c*]phenazine, tNCH = 4-*tert*-butyl-2-phenylpyridine) and ctDNA is proposed to involve a  $\pi$ -stacking interaction between the 1,2,3,4-tetrahydrophenazine moiety of the coordinated dppz ligand with the nucleobases of DNA.<sup>[9]</sup> Considering the non-emissive exciplexes formed between metal complexes and DNA,<sup>[8d,e,h]</sup> a notable example is Cu(TMpyP4).<sup>[17]</sup> This complex forms a groove-bound adduct with DNA which is non-emissive (in contrast to its intercalated DNA adduct which is emissive<sup>[17]</sup>) as a result of exciplex quenching caused by the axial coordination of water<sup>[17]</sup> or a donor atom of DNA.<sup>[8d]</sup> Herein, the exciplex formed between **1a** and ctDNA or AT-rich DNA shows an almost 200-fold enhancement in emission intensity and a significantly red-shifted emission maximum. Complex **1a** binds to ctDNA or AT-rich DNA through intercalation (Figure 2c), with the C<sup>^</sup>N<sup>^</sup>N<sup>^</sup> ligand plane inserting parallel to DNA bases. We suggest that the excited triplet state of **1a** is stabilized by  $\pi$ -interactions with A/T bases leading to a lowering of emission energy. In the cases of the other platinum(II) complexes **1b** and **1c**, there is no red-shift in emission energy upon their bindings with ctDNA (Figure S11). These results, together with ns-TRE measurements, revealed that the photophysical and emission properties of intercalating adducts are dependent upon the structures of the Pt<sup>II</sup> complex and nucleobases of NAs (see also ns-TRE of **1a** with p(dA)-p(dT) in Figure S10f). McMillin et al. also reported that the binding of [Pt(4'-NR<sub>2</sub>-trpy)(CN)]<sup>+</sup> (NR<sub>2</sub> = NMe<sub>2</sub>, N-pyrrolidinyl; trpy = 2,2':6':2''-terpyridine) with p(dA-dT) led to diminished quenching of emission by solvent and/or oxygen and an increase in emission excited-state lifetime.<sup>[18]</sup> Herein, no exciplex emission was detected in the binding between **1a** and p(rA)-p(rU). We suggest that, unlike B-form dsDNA, the A-form duplex conformation of dsRNA disfavors  $\pi$ -electronic interactions between the triplet excited state of **1a** and nucleobases. Thus, the intercalating adduct between **1a** and dsRNA does not give rise to a shift in emission maximum, which occurs at  $\lambda = 525$  nm and corresponds to the triplet emission of **1a**. The enhanced emission intensity detected is attributed to diminished quenching of the excited state by solvent molecules as a result of intercalation (Figure 2d). Experiments with other dsRNAs including three siRNAs with random sequences and an AU-rich dsRNA (r(AUA<sub>2</sub>U<sub>2</sub>A<sub>3</sub>U<sub>3</sub>A<sub>4</sub>U<sub>4</sub>A<sub>2</sub>)<sub>2</sub>) gave an emission enhancement of **1a** with an maximum wavelength at approximately  $\lambda = 525$  nm (Figure 2a,b, Figure S8c) and an emission profile similar to monomer emission. Of the dsRNA sequences employed, the detection of AU-rich dsRNA by **1a** was the most sensitive, where a concentration as low as 1  $\mu$ M in PBS could be detected by **1a** (Figure S8c). The presence of bovine serum albumin did not interfere in the binding as it did not affect the emission of **1a** (Figure S12). In the presence of dsDNA molecules, such as ctDNA, p(dA-dT), or p(dA)-p(dT), **1a** could also detect dsRNA down to 4  $\mu$ M based on an enhancement of emission at  $\lambda = 525$  nm, even in the presence of a fivefold excess of dsDNA (Figure S13).



The intriguing nucleic acid intercalation properties of pincer cyclometalated platinum(II) complexes prompted us to examine the binding interactions between **1a** and cancer-relevant DNA sequences. Figure S14a shows the effect of **1a** on the cleavage of a 23 bp dsDNA segment by topoisomerase I (TopoI), where the DNA segment is known to contain a high-affinity TopoI cleavage site.<sup>[19]</sup> Both **1a** and camptothecin (CPT, positive control) increased cleavage of this dsDNA substrate as indicated by the appearance of the 13-mer product. An oligonucleotide religation assay was also performed,<sup>[20]</sup> where **1a** inhibited TopoI-mediated religation of a complementary 13-mer (ON6) to the suicide cleavage complex as effectively as CPT did (Figure S14b).

The binding of TopoI with DNA has commonly been studied by performing electrophoretic mobility shift assay experiments with radiolabeled DNA.<sup>[21]</sup> We have tested whether the ternary complex (TopoI–DNA–**1a**) could be formed and traced in a native electrophoretic gel by using emission spectroscopy. As shown in the gel image in Figure 3a, orange-red emissive bands representing the binding complexes formed between **1a** and a specific oligomeric DNA substrate of TopoI<sup>[20]</sup> were detected (lanes 6, 8, 11, and 12; shown as intense white bands at bottom of gel). Upon incubation of TopoI (2.4 U  $\mu\text{L}^{-1}$ ) with **1a** (200  $\mu\text{M}$ ) and TopoI-specific DNA (460  $\mu\text{M}$ ), a shifted band with retarded electrophoretic mobility was also detected (lane 8, white circle). This orange-red emission band was not observed in the absence of DNA (lane 5) or **1a** (lane 7), or when TopoI was replaced with bovine serum albumin (lane 11) or heat-inactivated TopoI (lane 12). Replacing the TopoI-specific DNA substrate with non-specific ones in the assays, such as AT-rich (Figure S15, lane 5) or GC-rich (Figure S15, lane 4) DNA oligomers, did not give rise to a shifted emission band. Thus these results demonstrated the formation of a specific TopoI–DNA–**1a** ternary complex which could be traced by emission spectroscopy and the intercalating properties of **1a**.

We next examined whether **1a** could target TopoI in cancer cells. Band depletion assays<sup>[22]</sup> and immunocomplex of enzyme (ICE) bioassays<sup>[23]</sup> were performed to determine the levels of free TopoI enzyme and TopoI–DNA adduct, respectively. As shown in the band depletion assay in Figure 3b, treatment of SUNE1 cells with **1a** or CPT resulted in a marked decrease of free TopoI in the cell lysates obtained by alkaline denaturation compared to the control. Meanwhile, an ICE assay (Figure 3c) on the DNA and protein fractions showed that in untreated control cells, TopoI was only detected at the top of the CsCl gradient as free protein, whereas in cells treated with CPT or **1a**, TopoI was also found in the DNA fractions, suggestive of the formation of the covalent TopoI–DNA complex. Additionally, an alkaline comet assay (Figure S16) showed that the DNA cleavage events caused by treatment of the cells with **1a** were similar to those caused by CPT treatment.<sup>[24]</sup> Fluorescence microscopic analysis revealed that **1a** accumulated in the nuclei of human

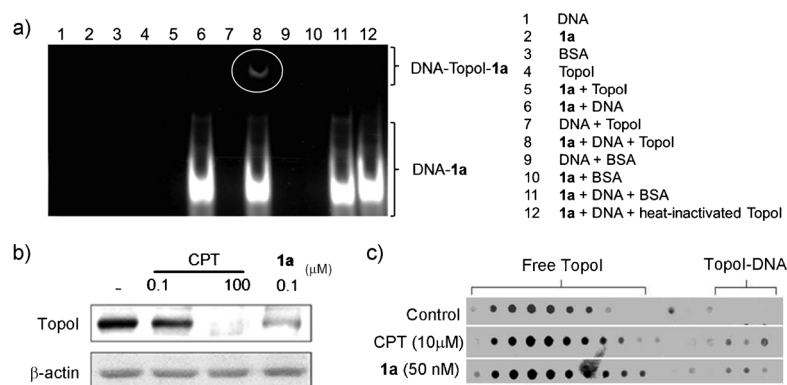


**Figure 3.** a) Gel-based detection of TopoI–DNA complex based on luminescent properties of **1a**. The mixtures containing different components were separated on a 6% native polyacrylamide gel which was subsequently examined under UV light. DNA: (5'-GAAAAAAGACTTGG-3' annealed with 5'-TAAAAATTTTTTCCAAGTCTTTTTTC-3'). b) Band depletion assay showing the decrease of free TopoI levels in the CPT- and **1a**-treated SUNE1 cells.  $\beta$ -actin levels were monitored as a control. c) ICE bioassays of the CPT- and **1a**-treated SUNE1 cells showing the formation of TopoI–DNA complex. The data presented are representative of at least two experiments.

oral epidermal carcinoma (KB) cells after incubation of the cells with the complex at 1  $\mu\text{M}$  for 6 h (Figure S17).

Stabilization of the TopoI–DNA cleavable complexes and subsequent DNA strain breaks would trigger programmed cell death. MTT assays (Table S2) indicated that **1a** is highly cytotoxic towards KB ( $\text{IC}_{50}$  = 9 nM), SH-5YSY (neuroblastoma,  $\text{IC}_{50}$  = 10 nM), NCI-H460 (non-small-cell lung carcinoma,  $\text{IC}_{50}$  = 110 nM), and SUNE1 (nasopharyngeal carcinoma,  $\text{IC}_{50}$  = 130 nM) cells after a 72 h cell treatment. However, **1a** displayed lower cytotoxicity towards normal lung fibroblast cell line CCD-19 Lu with an  $\text{IC}_{50}$  value of 18  $\mu\text{M}$ , which is 2000-fold higher than the  $\text{IC}_{50}$  value for KB cells. The cytotoxic  $\text{IC}_{50}$  value of **1a** towards a CPT-resistant KB cancer cell variant was found to be 65-fold higher than that towards the CPT-sensitive KB parental cells, suggesting that the cytotoxic effects of **1a** could be attributed to an inhibition of TopoI activity (Table S2). With the favorable in vitro cytotoxicity, we assessed the in vivo antitumor activity of **1a** in nude mice implanted with NCI-H460 lung cancer cells. Treatment of the mice with **1a** at 3  $\text{mg kg}^{-1}$  five times per week resulted in a statistically significant inhibition of tumor growth by 60% ( $p < 0.05$ ,  $n = 5$ , Figure 4) with no mouse death or mouse body weight loss (Figure S18a).

In summary, we have identified a class of luminescent pincer cyclometalated platinum(II) complexes, in which **1a**

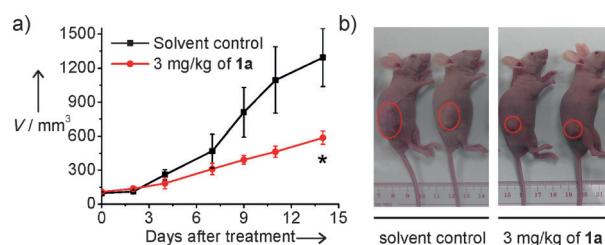


**Figure 4.** a) Average tumor volumes of mice bearing NCI-H460 xenografts after treatment with **1a** (3  $\text{mg kg}^{-1}$ ) or solvent through intratumoral injection. b) Representative photographs of mice after the 14 day treatment. \*,  $p < 0.05$  compared to solvent control. Tumor highlighted by red circle.

$[\text{Pt}(\text{C}^{\wedge}\text{N}^{\wedge}\text{N})(\text{C}\equiv\text{NtBu})]^+$  forms an emissive exciplex with double-stranded DNA. The sensitivity of the emission properties of the exciplex to nucleic acid structure is harnessed to differentiate between dsRNA and dsDNA. The stabilization of the TopoI–DNA–**1a** ternary complex with resulting DNA damage by **1a** contributes to the potent anticancer activities.

Received: May 19, 2014

Published online: July 15, 2014

**Keywords:** anticancer · DNA · exciplex emission · platinum · topoisomerase I

- [1] a) K. E. Erkkila, D. T. Odom, J. K. Barton, *Chem. Rev.* **1999**, *99*, 2777–2796; b) D. Wang, S. J. Lippard, *Nat. Rev. Drug Discovery* **2005**, *4*, 307–320; c) M. R. Gill, J. Garcia-Lara, S. J. Foster, C. Smythe, G. Battaglia, J. A. Thomas, *Nat. Chem.* **2009**, *1*, 662–667; d) F. R. Keene, J. A. Smith, J. G. Collins, *Coord. Chem. Rev.* **2009**, *253*, 2021–2035; e) A. M. Pizarro, A. Habtemariam, P. J. Sadler, *Top. Organomet. Chem.* **2010**, *32*, 21–56; f) H.-K. Liu, P. J. Sadler, *Acc. Chem. Res.* **2011**, *44*, 349–359; g) P. Wang, C.-H. Leung, D.-L. Ma, R. W.-Y. Sun, S.-C. Yan, Q.-S. Chen, C.-M. Che, *Angew. Chem.* **2011**, *123*, 2602–2606; *Angew. Chem. Int. Ed.* **2011**, *50*, 2554–2558; h) J. Suryadi, U. Bierbach, *Chem. Eur. J.* **2012**, *18*, 12926–12934; i) A. C. Komor, J. K. Barton, *Chem. Commun.* **2013**, *49*, 3617–3630; j) G. Barone, A. Terenzi, A. Lauria, A. M. Almerico, J. M. Leal, N. Busto, B. García, *Coord. Chem. Rev.* **2013**, *257*, 2848–2862; k) D.-L. Ma, H.-Z. He, K.-H. Leung, D. S.-H. Chan, C.-H. Leung, *Angew. Chem.* **2013**, *125*, 7820–7837; *Angew. Chem. Int. Ed.* **2013**, *52*, 7666–7682.
- [2] a) C. Metcalfe, J. A. Thomas, *Chem. Soc. Rev.* **2003**, *32*, 215–224; b) S.-W. Lai, C.-M. Che, *Transition Metal and Rare Earth Compounds, Vol. 241* (Ed.: H. Yersin), Springer, Berlin, **2004**, pp. 27–63; c) C. Rajput, R. Rutkaite, L. Swanson, I. Haq, J. A. Thomas, *Chem. Eur. J.* **2006**, *12*, 4611–4619; d) D.-L. Ma, C.-M. Che, S.-C. Yan, *J. Am. Chem. Soc.* **2009**, *131*, 1835–1846; e) A. Okamoto, *Chem. Soc. Rev.* **2011**, *40*, 5815–5828; f) M. R. Gill, J. A. Thomas, *Chem. Soc. Rev.* **2012**, *41*, 3179–3192; g) A. Granzhan, N. Kotera, M.-P. Teulade-Fichou, *Chem. Soc. Rev.* **2014**, *43*, 3630–3665.
- [3] a) C. S. Chow, K. M. Hartmann, S. L. Rawlings, P. W. Huber, J. K. Barton, *Biochemistry* **1992**, *31*, 3534–3542; b) H. R. Neenhold, T. M. Rana, *Biochemistry* **1995**, *34*, 6303–6309; c) E. Kikuta, S. Aoki, E. Kimura, *J. Am. Chem. Soc.* **2001**, *123*, 7911–7912; d) C. B. Carlson, O. M. Stephens, P. A. Beal, *Biopolymers* **2003**, *70*, 86–102; e) B. Tian, P. C. Bevilacqua, A. Diegelmann-Parente, M. B. Mathews, *Nat. Rev. Mol. Cell Biol.* **2004**, *5*, 1013–1023; f) H. Xu, Y. Liang, P. Zhang, F. Du, B.-R. Zhou, J. Wu, J.-H. Liu, Z.-G. Liu, L.-N. Ji, *J. Biol. Inorg. Chem.* **2005**, *10*, 529–538; g) C. B. Spillane, J. A. Smith, D. P. Buck, J. G. Collins, F. R. Keene, *Dalton Trans.* **2007**, 5290–5296; h) J. R. Thomas, P. J. Hergenrother, *Chem. Rev.* **2008**, *108*, 1171–1224; i) D. P. Buck, C. B. Spillane, J. G. Collins, F. R. Keene, *Mol. Biosyst.* **2008**, *4*, 851–854; j) S. Phongtongpasuk, S. Paulus, J. Schnabl, R. K. O. Sigel, B. Spingler, M. J. Hannon, E. Freisinger, *Angew. Chem.* **2013**, *125*, 11727–11730; *Angew. Chem. Int. Ed.* **2013**, *52*, 11513–11516; k) F. Li, E. J. Harry, A. L. Bottomley, M. D. Edstein, G. W. Birrell, C. E. Woodward, F. R. Keene, J. G. Collins, *Chem. Sci.* **2014**, *5*, 685–693.
- [4] B. Shirinfar, N. Ahmed, Y. S. Park, G.-S. Cho, I. S. Youn, J.-K. Han, H. G. Nam, K. S. Kim, *J. Am. Chem. Soc.* **2012**, *134*, 135, 90–93.
- [5] a) C. E. Crespo-Hernández, B. Cohen, P. M. Hare, B. Kohler, *Chem. Rev.* **2004**, *104*, 1977–2020; b) C. T. Middleton, K. de La Harpe, C. Su, Y. K. Law, C. E. Crespo-Hernández, B. Kohler, *Annu. Rev. Phys. Chem.* **2009**, *60*, 217–239; c) I. Vayá, T. Gustavsson, F.-A. Miannay, T. Douki, D. Markovitsi, *J. Am. Chem. Soc.* **2010**, *132*, 11834–11835.
- [6] a) H.-A. Wagenknecht in *Charge Transfer in DNA: From Mechanism to Application* (Ed.: H.-A. Wagenknecht), Wiley-VCH, Weinheim, **2006**, pp. 1–26; b) J. K. Barton, E. D. Olmon, P. A. Sontz, *Coord. Chem. Rev.* **2011**, *255*, 619–634.
- [7] a) K. Yamana, R. Iwase, S. Furutani, H. Tsuchida, H. Zako, T. Yamaoka, A. Murakami, *Nucleic Acids Res.* **1999**, *27*, 2387–2392; b) Y. Saito, K. Kugenuma, M. Tanaka, A. Suzuki, I. Saito, *Bioorg. Med. Chem. Lett.* **2012**, *22*, 3723–3726.
- [8] a) D. R. McMillin, F. Liu, K. A. Meadows, T. K. Aldridge, B. P. Hudson, *Coord. Chem. Rev.* **1994**, *132*, 105–112; b) A. Horváth, K. L. Stevenson, *Coord. Chem. Rev.* **1996**, *153*, 57–82; c) C. N. Pettijohn, E. B. Jochowitz, B. Chuong, J. K. Nagle, A. Vogler, *Coord. Chem. Rev.* **1998**, *171*, 85–92; d) D. R. McMillin, K. M. McNett, *Chem. Rev.* **1998**, *98*, 1201–1220; e) P. Lugo-Ponce, D. R. McMillin, *Coord. Chem. Rev.* **2000**, *208*, 169–191; f) D. K. Crites Tears, D. R. McMillin, *Coord. Chem. Rev.* **2001**, *211*, 195–205; g) D. R. McMillin, J. J. Moore, *Coord. Chem. Rev.* **2002**, *229*, 113–121; h) D. R. McMillin, A. H. Shelton, S. A. Bejune, P. E. Fanwick, R. K. Wall, *Coord. Chem. Rev.* **2005**, *249*, 1451–1459; i) S. D. Cummings, *Coord. Chem. Rev.* **2009**, *253*, 1495–1516; j) R. McGuire Jr., M. C. McGuire, D. R. McMillin, *Coord. Chem. Rev.* **2010**, *254*, 2574–2583.
- [9] C.-M. Che, M. Yang, K.-H. Wong, H.-L. Chan, W. Lam, *Chem. Eur. J.* **1999**, *5*, 3350–3356.
- [10] a) J. Fohrer, M. Hennig, T. Carlomagno, *J. Mol. Biol.* **2006**, *356*, 280–287; b) M. Cusumano, M. L. Di Pietro, A. Giannetto, P. A. Vainiglia, *Inorg. Chem.* **2007**, *46*, 7148–7153.
- [11] a) P. Wang, C.-H. Leung, D.-L. Ma, W. Lu, C.-M. Che, *Chem. Asian J.* **2010**, *5*, 2271–2280; b) J. Liu, C.-H. Leung, A. L.-F. Chow, R. W.-Y. Sun, S.-C. Yan, C.-M. Che, *Chem. Commun.* **2011**, *47*, 719–721.
- [12] a) E. Labourier, J.-F. Riou, M. Prudhomme, C. Carrasco, C. Bailly, J. Tazi, *Cancer Res.* **1999**, *59*, 52–55; b) W. A. Denny, B. C. Baguley, *Curr. Top. Med. Chem.* **2003**, *3*, 339–353; c) B. Montaner, W. Castillo-Ávila, M. Martinell, R. Öllinger, J. Aymami, E. Giralt, R. Pérez-Tomás, *Toxicol. Sci.* **2005**, *85*, 870–879; d) Y. Pommier, *Chem. Rev.* **2009**, *109*, 2894–2902.
- [13] J. Liu, R. W.-Y. Sun, C.-H. Leung, C.-N. Lok, C.-M. Che, *Chem. Commun.* **2012**, *48*, 230–232.
- [14] G. Cohen, H. Eisenberg, *Biopolymers* **1969**, *8*, 45–55.
- [15] K. Sandström, S. Wärmländer, M. Leijon, A. Gräslund, *Biochem. Biophys. Res. Commun.* **2003**, *304*, 55–59.
- [16] S.-W. Lai, M. C.-W. Chan, K.-K. Cheung, C.-M. Che, *Organometallics* **1999**, *18*, 3327–3336.
- [17] B. P. Hudson, J. Sou, D. J. Berger, D. R. McMillin, *J. Am. Chem. Soc.* **1992**, *114*, 8997–9002.
- [18] M. L. Clark, R. L. Green, O. E. Johnson, P. E. Fanwick, D. R. McMillin, *Inorg. Chem.* **2008**, *47*, 9410–9418.
- [19] Q. A. Khan, M. A. Elban, S. M. Hecht, *J. Am. Chem. Soc.* **2008**, *130*, 12888–12889.
- [20] S.-Y. Park, C.-H. Leung, Y.-C. Cheng, *Mol. Pharmacol.* **2008**, *73*, 1829–1837.
- [21] S. Shuman in *DNA Topoisomerase Protocols, Vol. 95* (Eds.: N. Osheroff, M.-A. Bjornsti), Humana, Totowa, **2001**, pp. 65–74.
- [22] S. D. Desai, T.-K. Li, A. Rodriguez-Bauman, E. H. Rubin, L. F. Liu, *Cancer Res.* **2001**, *61*, 5926–5932.
- [23] S. Antony, G. Kohlhausen, K. Agama, M. Jayaraman, S. Cao, F. A. Durrani, Y. M. Rustum, M. Cushman, Y. Pommier, *Mol. Pharmacol.* **2005**, *67*, 523–530.
- [24] T.-K. Li, P. J. Houghton, S. D. Desai, P. Daroui, A. A. Liu, E. S. Hars, A. L. Ruchelman, E. J. LaVoie, L. F. Liu, *Cancer Res.* **2003**, *63*, 8400–8407.